A Detailed Model on Kinetics and Microstructure Evolution during Copolymerization of Ethylene and 1-Octene: From Coordinative Chain Transfer to Chain Shuttling Polymerization

ARTICLE *in* MACROMOLECULES · JUNE 2014

Impact Factor: 5.8 · DOI: 10.1021/ma500874h

6 AUTHORS, INCLUDING:

Yousef Mohammadi
Petrochemical Research & Technology Company
20 PUBLICATIONS **267** CITATIONS
SEE PROFILE

mohammad mehdi Khorasani
Petrochemical Research & Technology Company
11 PUBLICATIONS **41** CITATIONS
SEE PROFILE

Florian J. Stadler
Shenzhen University
106 PUBLICATIONS **1,320** CITATIONS
SEE PROFILE

Macromolecules

Article

pubs.acs.org/Macromolecules

A Detailed Model on Kinetics and Microstructure Evolution during Copolymerization of Ethylene and 1-Octene: From Coordinative Chain Transfer to Chain Shuttling Polymerization

Yousef Mohammadi,[†] Mostafa Ahmadi,*[,‡] Mohammad Reza Saeb,[§] Mohammad Mehdi Khorasani,[†] Pianpian Yang,[$] and Florian J. Stadler*[,∥,⊥,#,&]

[†]Petrochemical Research and Technology Company (NPC-rt), National Petrochemical Company (NPC), P.O. Box 14358-84711, Tehran, Iran

[‡]Department of Polymer Engineering and Color Technology, Amirkabir University of Technology, Tehran, Iran

[§]Department of Resin and Additives, Institute for Color Science and Technology, P.O. Box 16765-654, Tehran, Iran

[∥]College of Materials Science and Engineering, Shenzhen University, Shenzhen 518060, P. R. China

[⊥]Shenzhen Key Laboratory of Special Functional Materials, Shenzhen 518060, P. R. China

[#]Shenzhen Engineering Laboratory for Advanced Technology of Ceramics, Shenzhen 518060, P. R. China

[&]Department of Semiconductor and Chemical Engineering, Chonbuk National University, Jeonju, South Korea

[$]Chonbuk National University, Baekjero 567, Deokjin-gu, Jeonju 561-756, South Korea

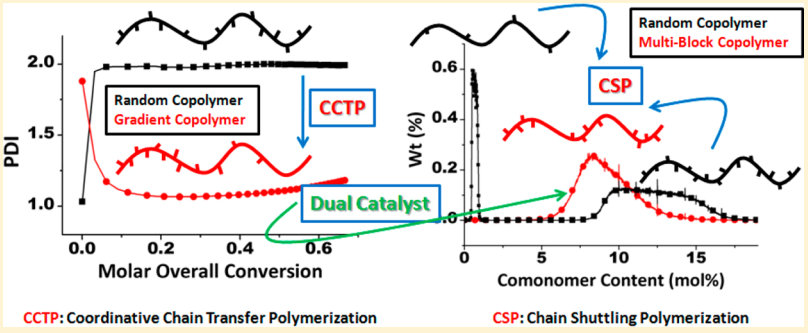

ABSTRACT: We introduce a theoretical model based upon the kinetic Monte Carlo (KMC) simulation approach capable of quantifying chain shuttling copolymerization (CSP) of ethylene and 1-octene in a semibatch operation. To make a deeper understanding of kinetics and evolution of microstructure, the reversible transfer reaction is first investigated by applying each of the individual catalysts to the reaction media, and the competences and shortcomings of a qualified set of CSP catalysts are discussed based on coordinative chain transfer copolymerization (CCTP) requirements. A detailed simulation study is also provided, which reflects and compares the contributions of chain transfer reversibility and other chain breaking reactions in controlling distribution fashion of molecular weight and chemical composition. The developed computer code is executed to capture developments in dead chain concentration and time-driven composition drift during CCTP. Also, the effect of chain shuttling agent (CSA) on the copolymerization kinetics is theoretically studied by simultaneous activation of both catalysts. In this way, it is attempted to make control over comonomer incorporation in the course of copolymerization. The molecular-level criteria reflecting copolymer properties, i.e., ethylene sequence length distribution and longest ethylene sequence length, as the signature of CSA performance, are virtually simulated in the presence and absence of hydrogen to capture an image on gradient copolymers in CCTP and blocks with gradually changing composition in CSP.

1. INTRODUCTION

Olefin-based polymers, namely homo- and copolymers of ethylene and/or propylene, account for about 50% of the polymers produced worldwide, highlighting their tremendous technological importance. Within the past decades, diverse investigations have been carried out to understand polyolefins landscape through comprehending their microstructural evolution.[1] From a chemical perspective, fine-tuning and controlling different features of architecture of differentiated materials is a complex task and necessitates precise design and optimization of catalytic systems.[2−6] Efforts in this field have led to development of new catalysts capable of precisely controlling the microscopic chain structure.

Received: April 27, 2014
Revised: May 31, 2014
Published: June 30, 2014

In the recent years, the synthesis of olefin block copolymers guaranteeing controlled molecular weight distribution (MWD) and chemical composition distribution (CCD) has become viable by living coordination polymerization (LCP).[7−9] In a LCP process, each catalyst precursor is responsible for the production of one chain, and diverse blocks can be synthesized by sequential addition of different monomers to the growing chain. The coordinative chain transfer polymerization (CCTP) is a cost-effective route combining LCPs and an appropriate chain transfer agent (CTA) in the reaction media.[10,11] The growing chains are capable of transfer from the catalyst center (live state) to the CTA (dormant state) via transalkylation. To fulfill this purpose, the rate of transfer reaction should be fast compared to propagation reaction; meanwhile, other chain breaking reactions like catalyst deactivation and β-hydrogen abstraction have to be negligible.[12,13] The other methodology referred to as chain shuttling polymerization (CSP) enables production of multi-block copolymers.[14−17] Olefinic block copolymers (OBCs) with hard and soft segments in the macromolecule's main chains (with low and high comonomer contents, respectively) follow the same concept.[16,17] This copolymerization strategy is based on the cooperative effect of two catalytic precursors: one having a lower ability to incorporate one of the comonomers, thus producing semicrystalline segments, and the other responsible for generation of amorphous low-melting-temperature fractions requiring sufficient capability of incorporating comonomer units.[18] The use of chain shuttling agent (CSA) facilitates exchange of growing chains between two catalysts, leading to sequential production of segments having high and low comonomer contents. The resulting multiblock copolymers combine benefits of both the high-melting-temperature mostly ethylenic blocks and the soft segments possessing a high comonomer content leading to a low glass transition temperature, giving the potential to commercially produce thermoplastic elastomers facilely (TPEs).[14−19] It was found that living catalyst systems with very small or no tendency toward chain transfer reactions can synthesize olefin block copolymers by sequential addition of monomers in a semibatch or tubular reactor.[7]

Despite the vital importance of olefin TPEs, the road to commercialization is typically long and requires an understanding of the microstructural evolutions during chain shuttling olefin copolymerization. To obtain a tailored microstructure with desirable distribution of hard and soft segments, a number of changing variables are required to be controlled.[20] The key, however, would be finding a compatible combination of CSA and a dual catalyst system to conduct alkyl−polymeryl exchange with an optimal frequency during growth of the chains. In their seminal paper, Arriola et al.[14] introduced a novel strategy to produce OBCs via chain shuttling copolymerization of ethylene and 1-octene. They examined a large number of catalysts and CSAs using high-throughput screening techniques to find the best combination of catalysts with significantly different monomer selectivities and compatible CSAs.[21] Nevertheless, further theoretical efforts are still needed for the realization and elucidation of the kinetics and mechanistic intricacies of chain shuttling reaction toward well-defined microstructures. Hustad et al.[22] proposed a mathematical model to investigate the effect of chain transfer reversibility on the MWD in semibatch CCTP. But despite this inspiring vision, they have not studied the effect of reversible chain transfer on development of chain microstructure in copolymerization reactions. Zhang et al.[23,24] developed a kinetic model of moments that predict molecular weight and overall copolymer composition during chain shuttling copolymerization. Later, they extended the ability of original model to capture an image of the average block structures such as average number of blocks per chain, average block length, and average number of linkage points between the soft and hard segments per chain.[25] The developed model could satisfactorily be applied to continuously stirred reactors to predict overall properties; however, it suffers from lack of ability to capture distributions of properties and, in particular, their time evolution. Anantawaraskul et al.[26] examined OBC chain microstructures using a Monte Carlo simulation. Through a parametric study they investigated the effect of different reaction probabilities on distribution of number of blocks per chain. Despite the fact that their model contains all the required basic kinetic steps, it ignores the hydrogen response difference of two catalysts involved.

In this study, we present a kinetic Monte Carlo (KMC) simulation algorithm capable of quantifying chain shuttling copolymerization of ethylene and 1-octene in a semibatch operation. To properly capture molecular-level events, we first visualize the effect of reversible transfer on the microstructure development and kinetics of copolymerization using each of the individual catalysts by virtue of chain architecture. In this regard, the competences and shortcomings of a qualified set of CSP catalysts are discussed based on CCTP requirements. The kinetic scheme and reaction rate constants are taken from the paper by Zhang et al. guaranteeing appropriate chain shuttling behavior of two distinct catalysts.[24,25] Then, the effect of CSA on the copolymerization is theoretically studied and discussed in the presence of both catalysts. The ethylene sequence length distribution (ESLD) and longest ethylene sequence length (LESL), as the molecular features, are virtually simulated in the presence and absence of hydrogen to capture an image on gradient copolymers in CCTP and ethylenic blocks with gradually changing composition in CSP.

2. KMC SIMULATION OF CHAIN SHUTTLING COORDINATION COPOLYMERIZATION

As a powerful and well-developed stochastically modeling approach, the KMC simulation method is capable of accurately imitating the polymerization processes of synthesizing complex macromolecules at the molecular level. Applying appropriate computing procedures, KMC can easily monitor the polymerization kinetics and describe the architecture of produced macromolecules in detail.

To establish a simulated version of the polymerization processes and construct a virtual reaction medium, type and concentration of all reactants existing inside the reactor at any given operational condition need to be precisely defined. In the beginning, an identification card is issued to each permitted molecule in the simulation volume. The predetermined mechanisms and reaction channels conducting and controlling all possible chemical and physical interactions and effective collisions among existing molecules in the simulation volume are managed and pursued by well-established computer codes. Performance and functionality of the designed algorithm for synthesizing virtual macromolecules along with the execution time of the corresponding computer codes are of vital importance and determine the extent, accuracy, and credibility of the final architectural information and the computational cost of this statistical approach.

Basically, to calculate the probability of a reaction channel happening at any given time interval, an appropriate criterion is defined mostly based on instantaneous reaction rates. The

dx.doi.org/10.1021/ma500874h | Macromolecules 2014, 47, 4778−4789

Scheme 1. Reaction Scheme Applied for Ethylene/1-Octene Chain Shuttling Copolymerization[24]

(1)	*Active-site formation*	$C_i \xrightarrow{k_a^i} C_i^*$
(2)	*Initiation*	$C_i^* + M_j \xrightarrow{k_i^i} R_{1,j}^i$
(3)	*Propagation*	$R_{n,k}^i + M_j \xrightarrow{k_{pkj}^i} R_{n+1,j}^i$
(4)	*Shuttling to virgin CSA*	$R_{n,k}^i + CSA \xrightarrow{k_{CS0}^i} D_{n,k} + C_i^*$
(5)	*Shuttling to polymeryl CSA*	$R_{n,k}^i + D_{m,j} \xrightarrow{k_{CS}^i} D_{n,i} + R_{m,j}^i$
(6)	*Chain transfer to hydrogen*	$R_{n,k}^i + H_2 \xrightarrow{k_{trH}^i} P_n + C_i^*$
(7)	*Thermal termination*	$R_{n,k}^i \xrightarrow{k_{th}^i} P_n + C_i^*$

i : Catalyst type
j,k : Monomer type (A: ethylene monomer and B: 1-octene comonomer)
C : Catalyst precursor
C^* : activated catalyst
$R_{n,k}$: Living chains with n repeat units ending in k-type monomer
$D_{n,k}$: Dormant chain with n repeat units ending in k-type monomer

allocated chance to each reaction channel is utilized to predict the system's behavior at that specific time interval. Afterward, the selected channel determines type and concentration of reactants having virtually reacted. Rearranging the concentration of reactants and products and updating the identification cards of various molecular species, the computer code adjusts time evolution through a stochastically determined increment. This computational algorithm is repeated until a preset reaction time is established.

Generally, if the polymerization process consists of N dominant elementary reaction channels, the m^{th} reaction is chosen in a given time interval from uniformly distributed random numbers in a unit interval, according to the following relationships:

$$\sum_{i=1}^{m-1} P_i \le r_1 \le \sum_{i-1}^{m} P_i$$

$$\mathrm{d}t = \frac{1}{\sum_{i=1}^{N} R_i} \ln\left(\frac{1}{r_2}\right) \quad (1)$$

where r_1 and r_2 are random numbers, P_i and R_i are the reaction rate probability and rate of reaction i, respectively, and dt is the time interval between two successive reactions.

In this work, Gillespie's algorithm was utilized to precisely determine the microstructure of ethylene/1-octene copolymers produced via coordinative chain transfer and chain shuttling coordination copolymerization processes.[27]

To synthesize ethylene/1-octene virtual copolymer chains, the KMC simulation of semibatch chain shuttling coordination copolymerization process of ethylene (monomer A) and 1-octene (comonomer B) was performed. To do this, the reaction scheme and copolymerization conditions suggested by Zhang et al. on mathematical modeling of chain shuttling copolymerization using dual catalysts were considered.[24] Applying the same simulation in the presence of only one of the catalysts leads to simulation of CCTP instead.

In our definitions, the first catalyst is identified by high comonomer consumption tendency. The second catalyst, on the contrary, has the main characteristic of only incorporating small amounts of comonomer in growing chains. The difference in comonomer content results in simultaneous formation of two distinct types of macromolecules, i.e., soft and hard α-olefin copolymer chains. In fact, CSAs actively exchange the role of growing and dormant chains in the reaction medium. The stochastically self- and cross-shuttling of active centers among different living and dormant chains, periodically experiencing ON and OFF situations, leads to the formation of multiblock polyethylene chains with alternating blocks with high and low comonomer contents. Obviously, the type and concentration of utilized CSA significantly influence the number and length of the soft and hard blocks constructing the produced OBC chains.

In this specific coordination copolymerization process, the architectural properties of the produced copolymer blocks are mainly influenced by the propagation and chain shuttling reaction channels. Because of the fact that the KMC simulation approach is capable of tracking, analyzing, and reporting all instantaneous and cumulative microstructural properties during the chain shuttling copolymerization of ethylene/1-octene, the proposed reaction channels are all considered to visualize a more comprehensive and reliable topological image of these novel polyolefin chains.

According to the proposed mechanism (Scheme 1), both catalysts are instantaneously activated and the addition of the first monomer/comonomer to an active center occurs immediately; i.e., the concentration of monomer-free active centers is always equal to zero.

The copolymerization process is triggered by the instantaneous activation of all existing catalyst molecules, spontaneously. Next, living chains are born through instantaneous initiation reaction channels. It is obvious that the instantaneous concentrations of ethylene and 1-octene molecules determine the type of the first monomer to be inserted into the monomer-free active sites.

Instantly generated living chains, which have taken the first monomer at time zero, are allowed to participate in propagation,

dx.doi.org/10.1021/ma500874h | Macromolecules 2014, 47, 4778−4789

Scheme 2. Simulation Flow Chart Proposed To Synthesize Ethylene/1-Octene Copolymers via Chain Shuttling Coordination Copolymerization

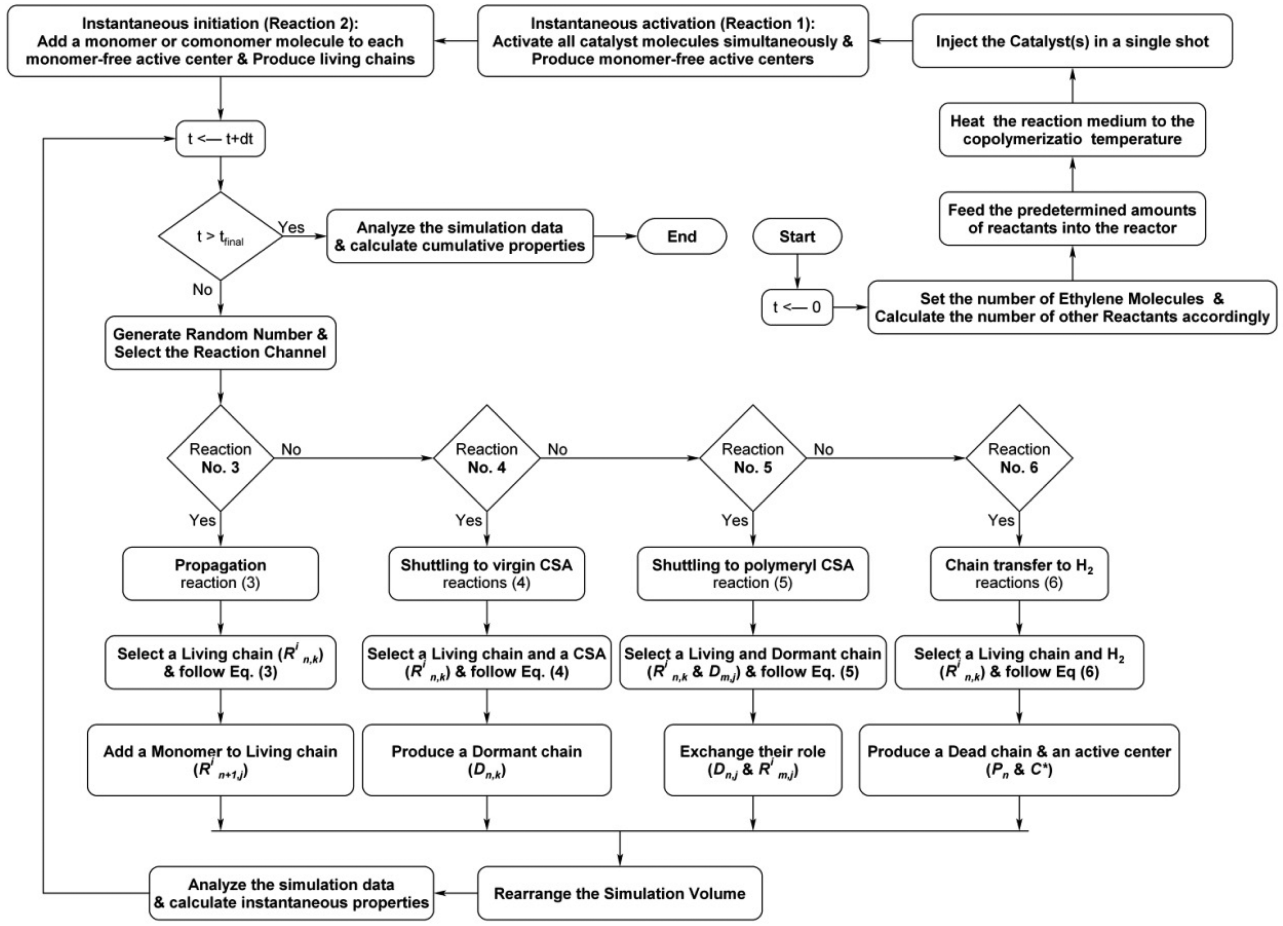

chain shuttling, or transfer to hydrogen reaction channels at the course of copolymerization. Whenever the propagation reaction is selected to happen, a living chain of type $R^1_{j,h}$ or $R^2_{j,h}$ should be selected. It is worth mentioning that a living chain of type $R^1_{j,h}$ denotes the jth growing chain ending in h-type monomer and attached to type 1 catalyst, i.e., a growing chain producing a soft block. It is obvious that four distinct types of living chains possibly exist in the simulation volume: (1) chains ending in ethylene repeating unit and attached to catalyst of type 1, (2) chains ending in 1-octene repeating unit attached to catalyst of type 1, (3) chains ending in ethylene repeating unit and attached to catalyst of type 2, and (4) chains ending in 1-octene repeating unit attached to catalyst of type 2.

In the present stochastic simulation work, the propagation of living chains is regulated by terminal model. Hence, for propagation of a type 1 living chain ending in monomer of type h, a selection probability was assigned to each growing chain of that type present in the simulation volume. A random number, $r1_{\text{living-chain}}$, was generated, and the m^{th} living chain of that type was selected for propagation providing the following criterion satisfied:

$$\sum_{j=1}^{m-1} p1_{j,h} \le r1_{\text{living-chain}} < \sum_{j=1}^{m} p1_{j,h}, \qquad p1_{j,h} = \frac{1}{NR1_h} \tag{2}$$

In this criterion, $p1_{j,h}$ is the selection probability of the jth living chain attached to catalyst of type 1 and ending in monomer of type h, while $NR1_h$ is the total number of living chains ending in monomer of type h and attached to catalyst of type 1 in the simulation volume.

To propagate the selected growing chain at the given time interval, the selection probabilities of ethylene and 1-octene monomers were determined based upon reaction rates. This allowed for determining the contribution of ethylene and 1-octene to the growing chains. According to classical statistical copolymerization equations, these probabilities are related to the reactivity ratios and instantaneous concentration of monomers.[28] Obviously, the proposed algorithm is also arranged to pursue a similar procedure to select and propagate a living chain of type 2 (currently synthesizing a hard block).

Undoubtedly, the origin of blocks in OBCs is due to the presence of chain shuttling agent in the reaction medium. In fact, both chain shuttling reaction channels, i.e., shuttling to either virgin or polymeryl CSA, are the main channels controlling block formation, frequency, and length. On the other hand, the blocks' architectural characteristics (length, comonomer content) are substantially determined by propagation step.

When the chain shuttling reaction channel is selected to happen, the synthesizing algorithm tries to find a living chain applying the same mechanism explained previously in section on propagation (Scheme 2). Afterward, a CSA molecule or a polymeryl CSA (a dormant chain) is selected to play the shuttling agent role. If shuttling reactions occur between a living chain and a CSA molecule, a dormant copy of the previously living chain with identical architecture is created and the living chain is deleted. Next, an ethylene or 1-octene monomer is

dx.doi.org/10.1021/ma500874h | Macromolecules 2014, 47, 4778−4789

inserted into the active center, previously having propagated the shuttled chain, instantly, to start living chain. On the other hand, in the case of a shuttling reaction via a polymeryl CSA, the active center attaches to the participated dormant chain and makes it alive.

It should be mentioned that the addition of an active center of type 1 to a dormant chain with a terminal soft block results in self-shuttling, while cross-shuttling or block type exchange takes place whenever a type 1 active center attacks a dormant chain ending in hard block. The same definitions and procedures are valid in living chains of type 2. The case of CCTP is simpler example of the situation described above, where in the presence of only one catalyst there is no possibility of cross-shuttling reaction.

To select a dormant chain for participating in all possible shuttling reactions, a selection probability was assigned to each dormant chain present in the simulation volume. A random number, $r_{\text{dormant-chain}}$, was generated and the m^{th} dormant chain was selected for shuttling reaction providing the following criterion satisfied:

$$\sum_{j=1}^{m-1} p_j \leq r_{\text{dormant-chain}} < \sum_{j=1}^{m} p_j, \qquad p_j = \frac{1}{ND} \tag{3}$$

In this criterion, p_j is the selection probability of the jth dormant chain and ND is the total number of dormant chains in the simulation volume.

Ultimately, the last reaction channel in chain shuttling α-olefin copolymerization is chain transfer to hydrogen terminating the growing copolymer chains. This reaction has a prominent role in controlling the average molecular weight and MWD. The selection mechanism of living chains to participate in terminating reaction channels is exactly similar to the aforementioned mechanism employed to simulate the propagation and shuttling channels. After chain transfer to hydrogen, a dead chain with a similar topology of terminated living chain is emerged. Again, the released active center attaches to a monomer or comonomer to form a new living chain.

To adequately quantify the instantaneous and cumulative properties of the produced OBC chains, the developed synthesizing computer code was implemented with appropriate mathematical procedures. The applied procedures are capable of analyzing and computing all microstructural and topological features of the simulated copolymers including MWD, CCD, ethylene sequence length distribution (ESLD), 1-octene dispersion, and the distribution of soft and hard blocks in the final products.

A total of 10^{11} ethylene molecules were seeded into the simulation volume, and the number of other reactants was computed based upon the copolymerization recipe proposed by Zhang et al.[24] The values of required kinetic parameters were extracted from the same work and listed in Table 1.

In a typical semibatch CCTP or CSP all reactants including solvent, ethylene, 1-octene, chain shuttling agent, cocatalyst components, and hydrogen are fed into the reactor at time zero. Afterward, the reaction medium is heated to the copolymerization temperature. The chain addition coordination copolymerization is initiated by a single shot of catalytic system into the reaction medium. To maintain the copolymerization pressure constant, ethylene is continuously loaded into the tank reactor. As a result, the concentration of ethylene is constant throughout the polymerization, while the comonomer and hydrogen are partially consumed in the reaction process. The required parameters for simulation conditions are collected from the aforementioned mathematical modeling work and shown in Table 2.

Table 1. Kinetic Parameters Used in CCTP and CSP Simulation[24]

parameter	catalyst 1	catalyst 2	unit
activation rate constant (k_a)	instantaneous	instantaneous	
initiation rate constant (k_i)	instantaneous	instantaneous	
homopropagation rate constant (k_{pAA})	1.0×10^5	1.0×10^4	L mol^{-1} s^{-1}
homopropagation rate constant (k_{pBB})	1.0×10^3	1.0×10^3	L mol^{-1} s^{-1}
shuttling to virgin CSA rate constant (k_{CS0})	1.0×10^6	1.0×10^6	L mol^{-1} s^{-1}
shuttling to polymeryl CSA rate constant (k_{CS})	1.0×10^6	1.0×10^6	L mol^{-1} s^{-1}
transfer to hydrogen rate constant (k_{trH})	5.0×10^3	50.0	L mol^{-1} s^{-1}
reactivity ratio of ethylene (r_A)	5.0	100	
reactivity ratio of 1-octene (r_B)	0.3	0.05	

Table 2. Parameters Used in Semibatch CCTP and CSP Simulation[24]

parameter	value	unit
initial concentration of ethylene	2.63	mol L^{-1}
solvent initial mass	1000	g
ethylene initial mass	200	g
1-octene initial mass	700	g
hydrogen initial mass	0.072	g
CSA initial mass	0.27	g
catalyst metal initial mass	1.50×10^{-4}	g
catalyst 1 molar ratio	0.5	

Each olefin block copolymer chain in the polymerization medium contains a number of soft and hard blocks with fixed lengths and architecture (i.e., static blocks). Except dead chains, the terminal block on the active side of a living or dormant chain is alive (i.e., a dynamic block), and its length and architecture vary at the course of copolymerization before experiencing a cross-shuttling event. Accordingly, a well-defined data storage structure should be designed to store all topological information necessary to completely visualize an OBC chain. To do this, a novel algorithm was proposed capable of storing all instantaneous characteristics of dynamic last block along with all cumulative information on static blocks on the same chain. This algorithm allowed the simulation of a statistically large sample size with a computationally cost-effective execution time.

The total simulation time, i.e. the CSP or CCTP reaction time (t_f), was assumed to be 600 s. A well-organized computer code, according to the proposed algorithm and flowchart presented in Schemes 2, was written in PASCAL programming language and compiled into 64-bits executable using FPC 2.6.2. A subroutine based on the Mersenne Twister algorithm was exploited to produce the required random numbers for the simulation. The random number generation subroutine satisfied the tests of uniformity and serial correlation with high resolution. The cycle length of the random number generator was $2^{19937}-1$. Simulations were performed on a desktop computer with Intel Core i7-3770K (3.50 GHz), 32 GB of memory (2133 MHz),

dx.doi.org/10.1021/ma500874h | Macromolecules 2014, 47, 4778−4789

under Windows 7 Ultimate 64-bit operating system. The runtime was approximately 9.24 h for all cases.

3. RESULTS AND DISCUSSION

Typically, the microstructure of OBCs is directly influenced by the nature of catalytic precursors incorporated. In this work, it is speculated that both the metallocene catalysts added into the system are able to produce chains with the most probable length and random comonomer distributions, as realized from Flory and Stockmayer equations, respectively. According to Arriola et al.,[14] catalysts suitable for chain shuttling polymerization may show a "hit" during the reaction, if reduction in molecular weight as well as narrowing molecular weight distribution takes place simultaneously in the presence of a compatible CSA. A fall in molecular weight and polydispersity index (PDI) has also been reported by others carrying out living radical polymerizations (LRPs).[29] There is ample evidence that LCP strategy similar to atom transfer radical polymerization (ATRP) results in only one chain per initiating site, based on reversible chain termination, while, on the basis of reversible chain transfer, it is possible to generate several chains from one active center in CCTP analogous to reversible addition−fragmentation transfer (RAFT).[30] Likewise, CSP is founded on polymeryl exchange between two catalysts mediated by a CSA trough reversible chain transfer reaction. Thus, depending on polymerization scheme and catalytic action of the used precursors, different microstructures can be gained from a single or dual catalyst in the assigned polymerization strategies. In this regard, it would be beneficial to start modeling from a simpler case, namely CCTP, to satisfactorily track the independent action of single catalytic precursor used for CSP. In the other words, the ability of catalysts routinely used for CSP in achieving tailored microstructures when used independently in CCTP could be recognized. With this target in view, the effect of CSA on kinetics of shuttling copolymerization was investigated pursing theoretical modeling of CCTP that features the role of metal alkyl as CTA on statistical copolymerization of ethylene and 1-octene. Attention is paid to put stress on the contribution of dead chain formation and/or reversibility of transfer reaction in the course of CCTP and CSP.

3.1. Modeling CCTP. In general, the introduction of CTA increases the number of chains formed and consequently decreases the overall molecular weight and at the same time obligates parallel growth of all chains leading to depletion of PDI. A fall in the number-average molecular weight (M_n) could be expected since the incorporated CTA has two alkyl groups with the potential of polymeryl−alkyl exchange reaction leading to formation of new chains. Figure 1 visualizes the effect of CTA on the evolution of M_n and PDI as a function of overall conversion in the semibatch polymerization scheme. For both catalysts, the reduction in the M_n and PDI is typical of the dominance of living polymerization and possibly minimization of other chain breaking reactions.[22] Slight upward turn in M_n at final conversions can be noticed for both catalysts. For the case of catalyst 1, compared to catalyst 2, the drop in PDI and M_n is less pronounced, and the overall polymerization trend resembles the behavior observed in the absence of CTA as reaction proceeds (Figure 1a). At the same time, PDI quickly drops below 2, followed by a steady convergence back to 2 at higher conversions, as observed elsewhere experimentally.[14,22] In the case of catalyst 2 (Figure 1b), M_n increases monotonically but reaches a value considerably lower than what would be obtained without CTA. This finding can be explained by the fact that the initial transfer to virgin CTA occurs when chains are extremely short. PDI

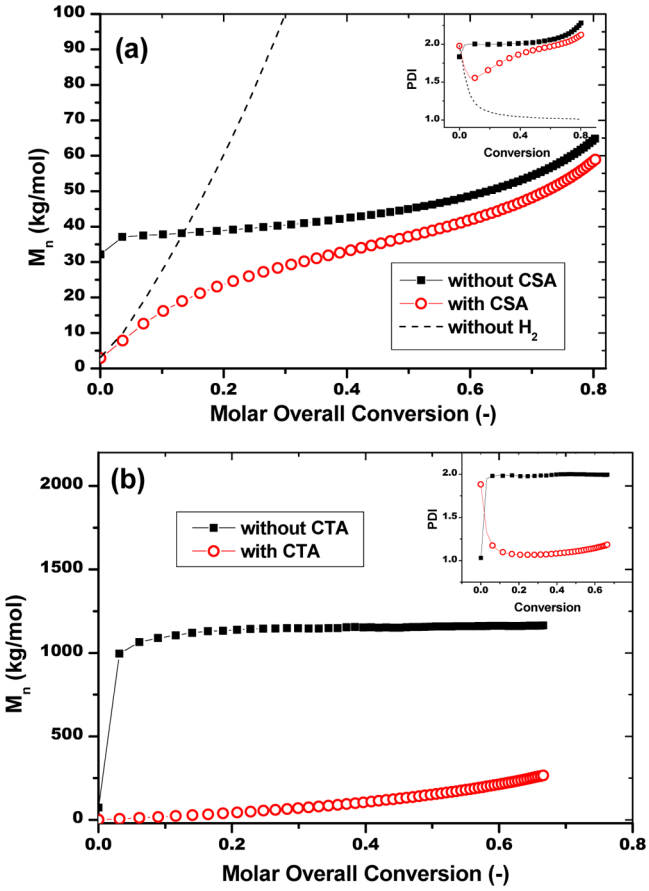

Figure 1. Effect of CTA on evolution of M_n (main plot) and PDI (inset) against overall conversion: (a) catalyst 1 with (solid lines) and without hydrogen (dotted lines); (b) catalyst 2.

decreases significantly at the initial stages of polymerization with minor increase about the final conversions. Britovesk et al. have reported similar experimental trends by producing oligomers with PDIs close to unity.[12,13]

There are several possibilities that influence kinetic features of living polymerization, as observed in Figure 1. It is believed that the instantaneous consumption of CTA avoids wild formation of long chains in the beginning of polymerization and obligates parallel propagation of growing chains. Moreover, CTA controls the synchronous growth through dynamic exchange of polymeryl chains between living state attached to catalyst and dormant state bearing the CTA. Lastly, formation of dead chains would fade the living features away, mostly through unavoidable transfer to monomer and β-hydrogen abstraction.[31,32] In the rest of this section, we will check these mentioned possibilities.

Figure 2 compares reduction in concentration of CTA beside development of dormant chains at the initial stages of reaction for two catalysts. For both cases the consumption of virgin CTA and formation of polymeryl-substituted CTA takes place in a few seconds. The fast initial transfer observed by the model development governed the livingness of polymerizations by reversible chain transfer.

The frequency of dynamic exchange of polymeryl group can be recognized by comparing chain propagation to chain transfer rate:

$$R_p = k_p[M][\lambda_0] \quad (4)$$

dx.doi.org/10.1021/ma500874h | Macromolecules 2014, 47, 4778−4789

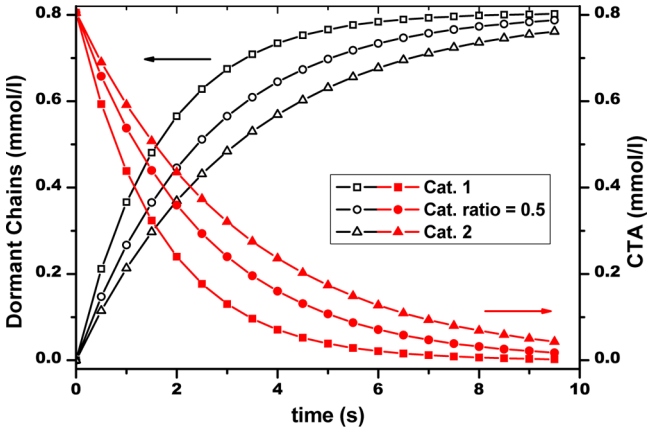

Figure 2. Consumption of CTA and formation of dormant chains at the initial stages of reaction.

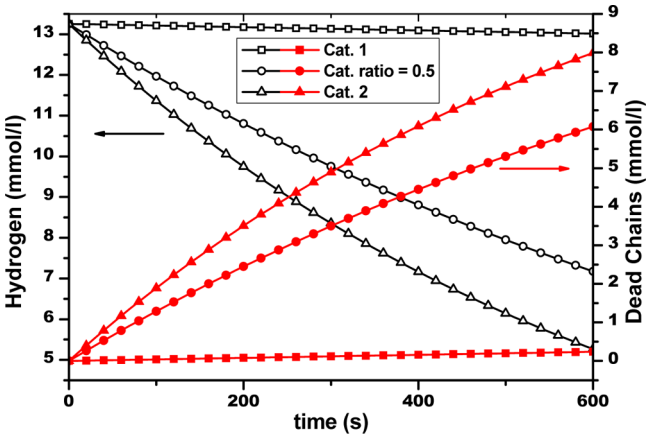

Figure 3. Consumption of hydrogen and formation of dead chains during reaction course.

$$R_{CT} = k_{CS}[CTA][\lambda_0] \quad (5)$$

where $[M] = [M_1] + [M_2]$ is the total monomer concentration, $[\lambda_0] = [\lambda_{01}] + [\lambda_{02}]$ is the zeroth moment of total live chains (λ_{0i} is the zeroth moment of live chains ended in monomer i), and [CTA] represents the concentration of dormant chains assuming fast consumption of transfer agent. The overall propagation and chain transfer rate constants can be defined as follows:

$$k_p = k_{p11}f_1\varphi_1 + k_{p12}f_2\varphi_1 + k_{p21}f_1\varphi_2 + k_{p22}f_2\varphi_2 \quad (6)$$

$$k_{CS} = k_{CS1}\varphi_1 + k_{CS2}\varphi_2 \quad (7)$$

where $f_1 = [M_1]/([M_1] + [M_2])$ is the molar fraction of ethylene and $\varphi_1 = [\lambda_{01}]/([\lambda_{01}] + [\lambda_{02}])$ is the molar fraction of live chains with terminal ethylene unit. Assuming steady-state conditions for growing chains with different terminal groups ($k_{p12}[M_2][\lambda_{01}] = k_{p21}[M_1][\lambda_{02}]$), one can calculate φ_1:

$$\varphi_1 = \frac{k_{p21}[M_1]}{k_{p21}[M_1] + k_{p12}[M_2]} \quad (8)$$

In these equations, k_{p12} is the rate constants for propagation reaction consisting $[M_2]$ and $[\lambda_{01}]$ while k_{CS1} represents rate constant for transfer to CTA from a live chain with ethylene as the terminal unit. Following these straightforward calculations, we come to the conclusion that the chain propagation is 72 and 32.9 times more frequent than the reversible chain transfer reaction for catalyst 1 and 2, respectively. Hustad et al.[24] have studied the effect of reversibility in CCTP for the ratio of propagation to transfer reactions of 100 up to 10 000. They stated that even for the case with propagation rate 100 times faster than reversible chain transfer rate, linear increase in M_n and PDI near 1.1 could be achieved. This conclusion is reasonable taking into account the high value of intrinsic molecular weight they have considered, rising from the minimal background transfer reactions. In this work, however, the possibility of chain transfer is indeed higher for both catalysts activated in the simulation space, especially for catalyst 1. The difference lies in the last kinetic requirement discussed above that is the formation frequency of terminated chains. Figure 3 reveals the rate of hydrogen consumption next to the rate of dead chain formation. Hydrogen consumption, which is responsible for formation of dead chains through chain transfer to hydrogen reaction, exists for both catalysts; however, it is more pronounced for catalyst 1. This reaction is responsible for the increase of PDI at later stages of reaction since the fully grown dead chains outnumber the summation of dormant and growing chains (see Figure 1).[31,32] Such circumstance can be avoided by removing hydrogen from the reaction conditions. The evolution of M_n (linearly increased) and PDI (decreased down to 1.01) in the absence of hydrogen with catalyst 1 is depicted by dotted lines in Figure 1a. Nevertheless, the occurrence of other inevitable inherent transfer reactions might account for deviation observed from an ideal living behavior.[22] It is worth mentioning that by progress of reaction and depletion of comonomer concentration in feed, the contributions of slow propagation terms (involving comonomer) in eq 6 exhaust, and therefore, the overall propagation rate constant increases. This alteration results in minor upward turn in M_n at very high conversions.

The simulation results implemented for MWD reveal that not only the reversibility of chain transfer reaction but also the frequency of other chain breaking reactions are responsible for control of MWD, and a successful CCTP catalyst should satisfy both kinetic requirements. There are limited experimental reports on the comonomer incorporation along growing copolymer chains in the course of CCTP and CSP.[33−39] Kuhlman et al. report on faster coordinative chain transfer after ethylene insertion rather than after 1-hexene insertion, which can be related to the presence of the butyl branch at the β-position of 1-hexene units which slows down the polymeryl exchange reaction.[39]

From a molecular standpoint, modeling or robust theoretical interpretations give more detailed information in this context. However, the success or failure of theoretical modeling is strongly dependent on the nature of implemented model and the skill of computer code developer. For example, the moment model developed by Zhang et al.[24] addresses overall copolymer composition neglecting terminal group impact on the reversibility of chain transfer reaction.

In semibatch synthesis of olefinic copolymers using classical coordination catalytic systems, a substantial composition drift in comonomer content of chains produced at different stages of reaction is inevitable if the comonomer incorporation is considerable. This makes the overall *interchain* comonomer distribution to diverge from random instantaneous distribution described by the Stockmayer equation. The gradient copolymer chain formation is a well-known microstructural feature that appears in living polymerization systems. By extending lifetime of growing chains caused by CTA, it is expected that chains

dx.doi.org/10.1021/ma500874h | *Macromolecules* 2014, 47, 4778−4789

experience the same evolving environment and composition drift along backbone.[40−42] Correspondingly, the length of monomer sequences in the chain varies from one end to the other. Despite the fact that this type of *intrachain* distribution cannot be characterized by the current analytical equipment, it can be inferred from other chain characteristics. In fact, by even distribution of comonomer units between all chains, CCD should become remarkably narrower despite the gradient *intrachain* distribution of comonomers.

Figure 4 displays the effect of CTA on the final distribution of comonomer content and evolution of cumulative comonomer content over polymerization time, which is achieved by stochastic simulation based on KMC. For both catalysts activated, the effect of CTA on cumulative comonomer content is negligible. This arises from the fact that the influence of terminal group on reversibility of transfer reaction has not been considered in the original model.[24] In the case of CTA-free copolymerization with catalyst 1 possessing superior ability of comonomer incorporation, composition drift follows an ascending trend by time; evidently, the cumulative comonomer content varies from 16% to almost 10% (inset in Figure 4a). One would expect that by introduction CTA the *interchain* composition drift should switch to *intrachain* drift along the backbone and CCD become narrower. However, modeling results reveal that the influence of CTA on CCD is not significant. This observation denotes that the formed chains do not really have similar gradient comonomer distributions. In this case the reversible transfer to CTA is only 12 times faster than the irreversible transfer to hydrogen ($R_{CT}/R_{trH} = k_{CT}[CTA]/k_{trH}[H_2]$). It can be concluded that by frequent production of dead chains via transfer to hydrogen at different stages of polymerization, chains of different gradient *intrachain* comonomer distributions are created. Thus, the gradient copolymers produced at different stages of polymerization undergo a noticeable *interchain* composition drift, which can be prevented by not using hydrogen for molar mass control. Figure 4b illustrates the effect of dead chain formation via transfer to hydrogen reflecting from the obtained CCD. As expected, CCD becomes strictly narrower upon removal of dead chain formation. This behavior implies that all chains having almost the same length (dotted lines in Figure 1a) experience similar *intrachain* composition drift. The inset in Figure 4b displays the instantaneous comonomer consumption (or local copolymer composition) against evolution of molecular weight. The gradient comonomer distribution along the backbone can be deduced from such a depiction of evolving polymerization behavior. The local comonomer content varies from 16% to 6% from one end of the chain to the other. The obtained simulation results reveal that hydrogen, acting as an irreversible transfer agent, can be used to manipulate the microstructure of polymer produced ending in a controlled CCD over polymerization course. Nonetheless, even in the absence of hydrogen, other inherent chain transfer reactions can have a large influence on the CCD, which can be tuned by devised catalyst selection.

In the case of catalyst 2 with lower tendency for comonomer incorporation, variation of comonomer content by time is not significant and, hence, composition drift is negligible (Figure 4b). Since the *interchain* composition drift in the absence of CTA do not affect cumulative comonomer distribution, CCD obeys the narrow distribution according to the Stockmayer equation. Given these conditions, one would anticipate negligible *intrachain* composition drift and, therefore, no influence on CCD upon introduction of CTA. On the other hand, simulations

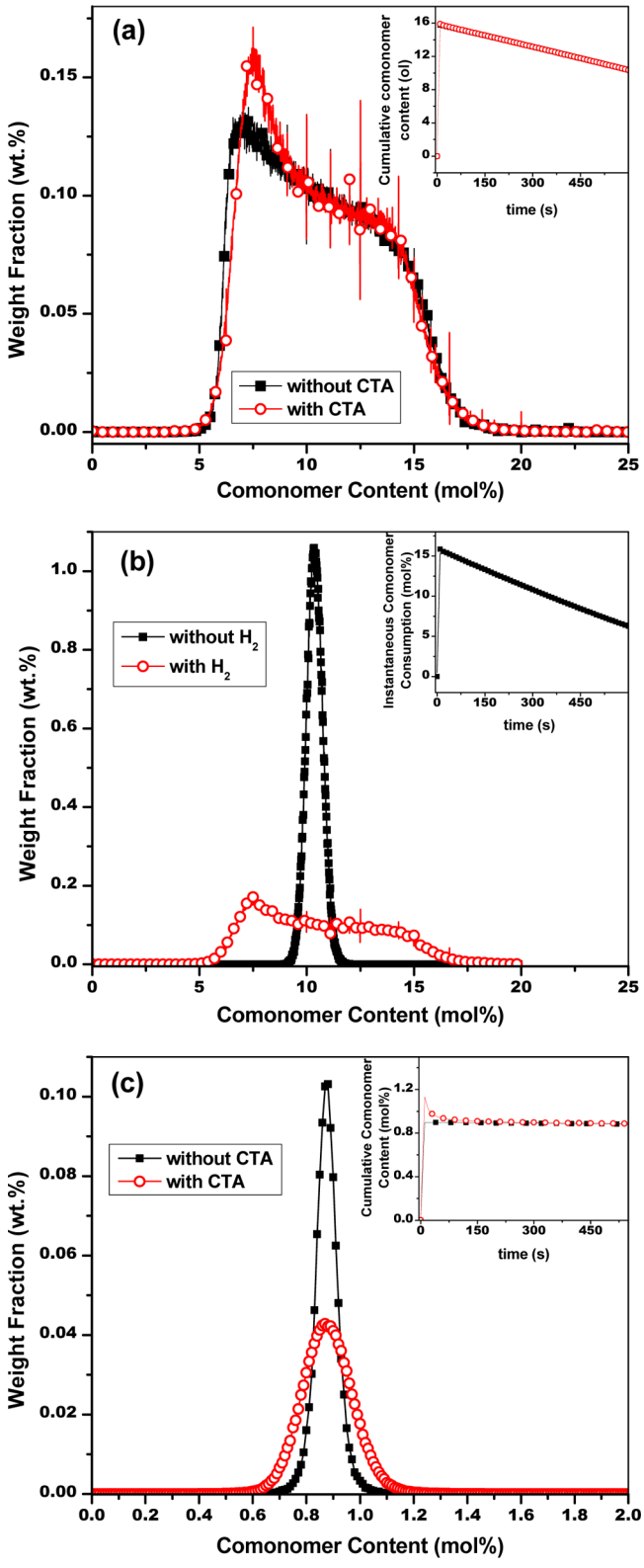

Figure 4. (a) Effect of CTA on end of batch CCD for catalyst 1; inset: variation of cumulative comonomer content. (b) Effect of hydrogen on end of batch CCD for catalyst 1 in the presence of CTA; inset: instantaneous comonomer consumption. (c) Effect of CTA on end of batch CCD for catalyst 2; inset: variation of cumulative comonomer content.

dx.doi.org/10.1021/ma500874h | *Macromolecules* 2014, 47, 4778−4789

predict broadening of CCD that can be related to the fact that CTA increases the number of formed chains, which in turn enhances the diversity in *interchain* comonomer distribution.

3.2. Modeling CSP. The kinetic simulations described above reveal that the introduction of reversible chain transfer reaction brings about living polymerization characteristics into the coordination polymerization of olefins. Coordinative chain transfer in the presence of dual catalysts may result in shuttling of the growing chains between precursors. After each transfer to CSA, there is the possibility of self-shuttling back to the same catalyst or cross-shuttling to the other one. In this way, subsequent segments along a single chain might be originated from different catalysts. Examples include simultaneous application of catalysts with different reactivity toward dissimilar monomers,[16,17] or catalysts with different stereospecificity in homopolymerization of α-olefins,[19] combination of late metallocene catalysts capable of chain walking leading to hyperbranched microstructure and metallocene catalysts exclusively making linear chains in homopolymerization of ethylene,[43] and utilizing catalysts with drastically dissimilar ability of comonomer incorporation in ethylene/α-olefins copolymerization.[14,20,39] The detailed microstructure of multiblock chains produced upon cooperation of two catalysts can be better estimated regarding the individual function of each catalyst in separate CCTP reactions. In this section, the cooperative function of catalysts individually treated before is theoretically investigated executing a computer code developed based on KMC.

Figure 5 shows the effect of CSA on the evolution of M_n and PDI under the conditions provided in Table 3. In the absence of CSA, the final product should have bimodal MWD, as the two catalysts produce chains of widely separated lengths, independently. The shape of bimodal distribution is the signature of relative activity and chain length of polymers produced by each catalyst ending in high PDI values appeared. The obtained results after introduction of CSA are not averages from polymers separately produced over two catalysts. Contrary, each of the catalysts governs some specific properties. By each time shuttling of growing chains to catalyst 1, there is a considerable probability of chain transfer to hydrogen and formation of dead chain. So, catalyst 1 dominates chain breaking reactions and evolution of molecular weight. In parallel, PDI decreases significantly, since catalysts collaborate in parallel growth of all chains toward narrower MWD. As explained before, there is a 1 in 13 chance that the transfer from catalyst 1 leads to an irreversible transfer to hydrogen and, consequently, formation of dead chains (middle lines in Figures 2 and 3). It can be concluded that catalyst 1 is in charge for slight increase of PDI at the final stages of polymerization. The dotted lines in Figure 5 reveal the effect of removing dead chain formation by subtracting hydrogen from reaction conditions. As expected, M_n increases linearly at the initial stages of reaction headed for much higher values and PDI decreases continually down to 1.01, which is typical of ideal living systems. It should be considered that ideal living behavior might not be always desirable, as for achieving chain lengths suitable for practical applications at least one of the utilized catalysts should break the rule and avoid formation of too long chains to keep the rheological properties in a range, where conventional polymer processing is possible.

Despite the fact that formation of dead chains disturbs precise control over MWD, the more important feature in synthesis of OBCs is engineering the distribution of comonomer units along the chains. Figure 6 shows the effect of CSA on the end of batch CCD and the evolution of cumulative comonomer content. The

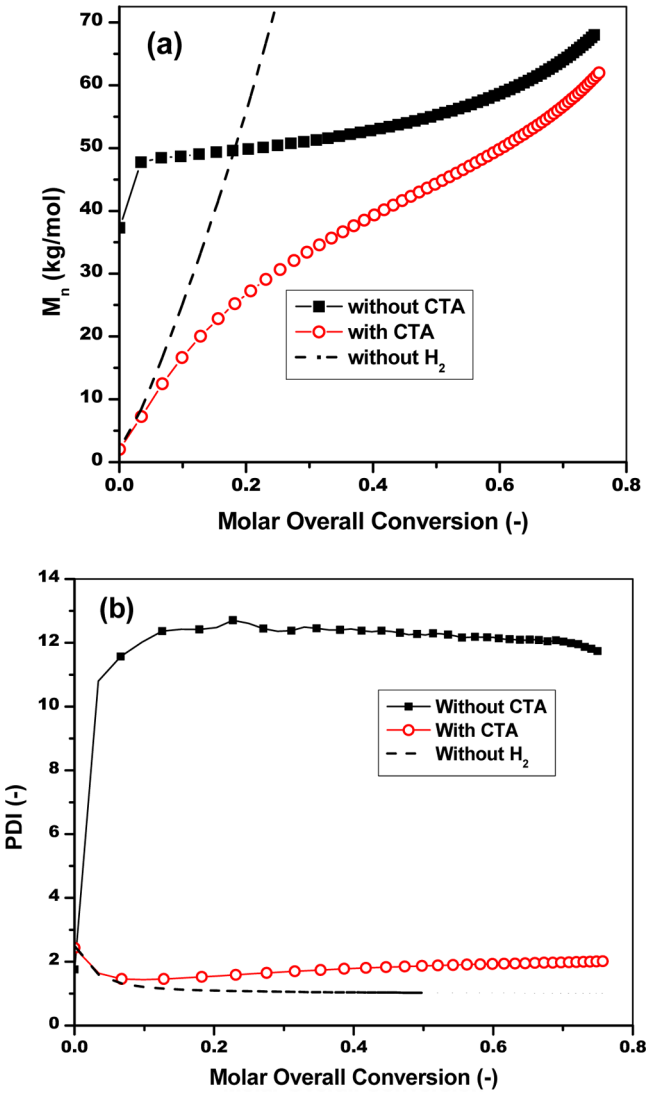

Figure 5. Effect of CSA on evolution of (a) M_n and (b) PDI against overall conversion (dotted lines represent CSP in the absence of hydrogen).

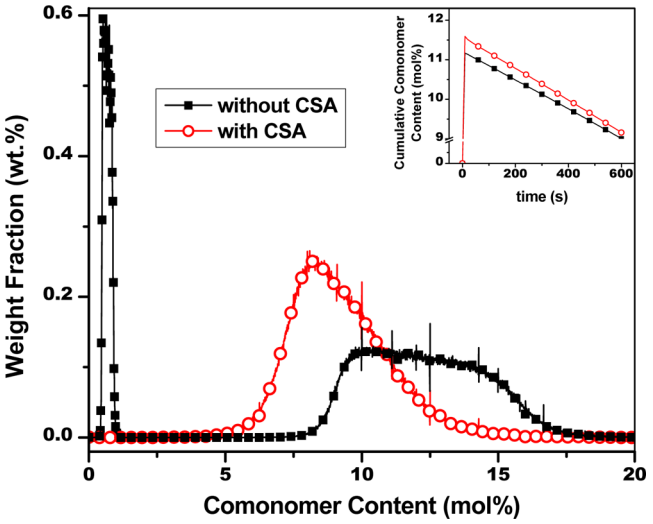

Figure 6. Effect of CSA on the end of batch CCD; inset: variation of cumulative comonomer content in polymerization course.

dx.doi.org/10.1021/ma500874h | *Macromolecules* 2014, 47, 4778−4789

considerable different tendencies of catalysts toward comonomer incorporation lead to discernibly bimodal CCD. Contrary to M_n, the obtained cumulative comonomer content after insertion of CSA is the average of comonomers incorporated by each of the catalysts. Because of identical transfer rate constants, after shuttling to each catalyst, they have the chance to integrate comonomer according to their own rate and the cumulative comonomer content does not vary.

Selection of different shuttling rate constants may favor one catalyst in living state and results in change of the overall comonomer incorporation. This behavior is not unexpected, as the spatial constraints from a bulky ligand may exclude one catalyst from frequent shuttling. The subtle effect of shuttling reaction on the chain microstructure can be recognized by study of CCD variation upon inclusion of CSA. The widely separated bimodal CCD curve turns into a unimodal curve, even narrower than the one could be independently attained from catalyst 1. The chains with extensively different comonomer contents have become discrete and evenly unified in succeeding blocks of high and low comonomer content along the backbone.

The blocky chains produced at different stages of polymerization still contain *interchain* composition drift due to the consumption of hydrogen. The broad CCD turns into a sharp curve by avoiding the time driven composition drift by removal of hydrogen, as revealed in Figure 7. This observation implies

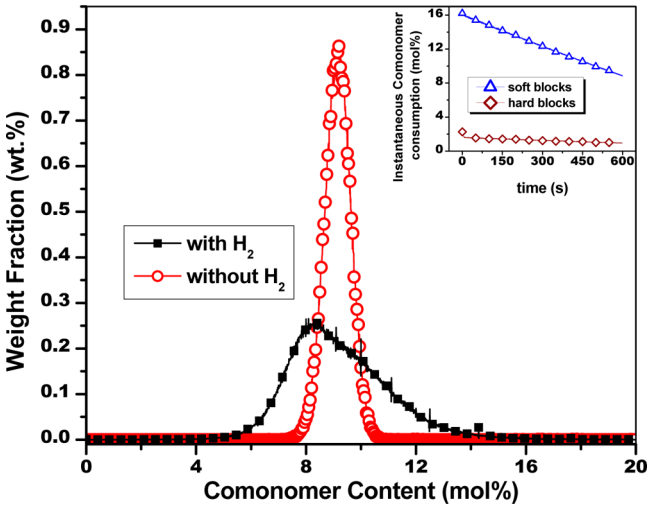

Figure 7. Effect of hydrogen removal on the end of batch CCD obtained in CSP; inset: variation of instantaneous comonomer consumption by each catalyst against reaction time in the absence of hydrogen.

that all chains should have similar gradient comonomer distribution. Each individual block has a homogeneous comonomer distribution because of the short time between two consecutive shuttling and transfer reactions. In other words, the *intrachain* gradient distribution arises from the gradually appearing composition drift between subsequent blocks. The inset in Figure 7 shows the instantaneous comonomer consumption by catalysts 1 and 2, representing the gradient change in comonomer content of respectively soft and hard blocks along the backbones as chains grow, in the absence of hydrogen. This structural composition drift compared to the case observed in CCTP is weaker for catalyst 1 and particularly far stronger for catalyst 2. In fact, catalyst 1 changes the feed composition enough to impose discernible composition drift in the hard blocks as well.

3.3. Remarks on the Microstructure. In the previous sections we studied the effect of reversible transfer on the evolution of MWD and CCD and probable emerge of gradient comonomer distribution in CCTP and CSP. In this section, some other microstructural aspects are addressed to enlighten our discussion. ESLD and LESLD are two of the important microstructural characteristics that affect the physical properties of copolymers to great extents.[16,44,45] They can also provide insight into the homogeneity of comonomer distribution along the chain. Figure 8 depicts variation of LESLD as the main plot and ESLD as the inset upon introduction of CTA in CCTP. For both catalysts no distinguishable effect on ESLD could be recognized. For the case of catalyst 1 even LESLD does not change significantly. In fact, complicated effects of chain length reduction and parallel emergence of inter- and intrachain composition drift compensate each other. In the case of catalyst 2, however, the more sensitive parameter of LESLD moves to lower values due to the significant reduction in the overall M_n. The effect of removing hydrogen from CCTP using catalyst 1 is illustrated in Figure 8c. The elimination of chain breaking reactions gives rise to production longer chains; however, since comonomer incorporation dictates length of majority of ethylene sequences, it shows no noticeable effect on ESLD. Conversely, the LESLD noticeably shifts toward higher values.

Figure 9 displays the evolution of ESLD and LESLD upon introduction of CSA in CSP. The independent action of catalysts in the absence of CSA leads to a physical blend having bimodal ESLD and LESLD as magnified in the insets. In the presence of CSA the ethylene sequences and more specifically the longest ones from different catalysts are disrupted and merged into one chain. The obtained unimodal distributions are the weighted summation from different blocks, which can be further tuned by controlling the length of soft and hard segments. However, physical properties of OBCs, e.g. melting and crystallization temperatures, are mainly determined by the microstructural properties of the discrete blocks and not the whole chain.[16,44,45] The effect of reaction conditions on the microstructure of different blocks will be presented in a sequel paper.

4. CONCLUSIONS

Coordinative chain transfer and chain shuttling polymerizations are established on the same idea of reversible chain transfer reaction. However, no comparative theoretical study has been conducted to explore capabilities of these two systems given their similar kinetic features. In this work a KMC model is developed to investigate kinetics and microstructure evolution during CSP pursing theoretical modeling of CCTP that features the role of metal alkyl as CTA on statistical copolymerization of ethylene and 1-octene in a semibatch process. It is shown that formation of dead chains through irreversible chain breaking reactions leads CCTP to diverge from ideal living polymerization features and increase PDI at the final stages of reaction. Frequent irreversible transfer reactions are also responsible for simultaneous formation of interchain composition drift and widening of CCD. Introduction of CSA in a dual catalytic system of CSP turns bimodal MWD and CCD into unimodal curves. However, same deviation is expected during cooperative function of two catalysts; i.e., formation of dead chains leads to similar increase in width of MWD and CCD. Removal of hydrogen from reaction system and, therefore, preventing dead chain formation clearly brings about living polymerization characteristics, namely, linear increase of M_n and decrease of PDI down to values near unity and, at the same time, formation of similar gradient comonomer

dx.doi.org/10.1021/ma500874h | *Macromolecules* 2014, 47, 4778−4789

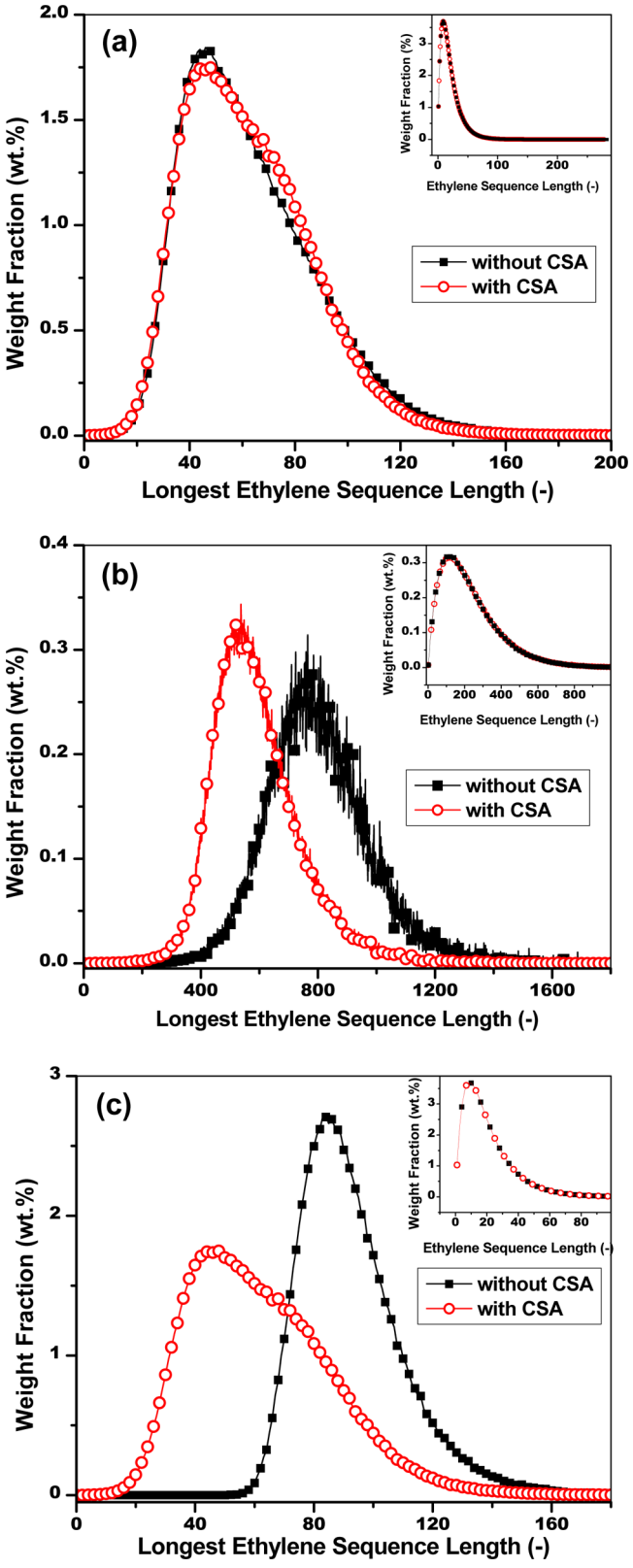

Figure 8. Effect of transfer reaction on the LESD obtained in CCTP for (a) catalyst 1, (b) catalyst 2, and (c) catalyst 1 in the absence of hydrogen; insets: ESLD achieved at the same conditions.

distribution along chains in both systems. However, since the ratio of reversible transfer to propagation reaction rate determines the blocky structure, they are less affected by the dead chain formation reactions.

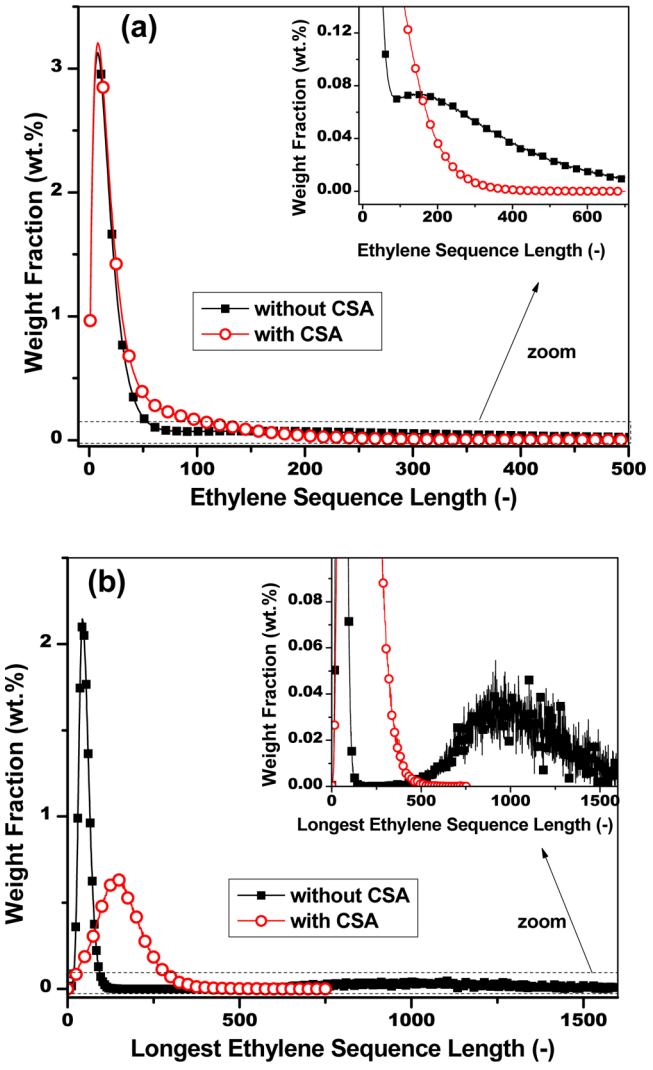

Figure 9. Variation of ESLD (a) and LESLD (b) upon introduction of CSA in CSP; insets: magnified regions.

Finally, the bimodal LES distribution achieved by simultaneous application of two catalytic system turns into a broad unimodal curve upon introduction of CSA.

AUTHOR INFORMATION

Corresponding Authors

*E-mail mo.ahmadi@aut.ac.ir (M.A.).
*E-mail fjstadler@szu.edu.cn (F.J.S.).

Notes

The authors declare no competing financial interest.

ACKNOWLEDGMENTS

M.A. and F.J.S. thank Prof. Dr. Christian Bailly for the continued support and hospitality beyond the working time of both at Université catholique de Louvain, which made the discussions leading to this article possible. F.J.S. thanks National Research Foundation of Korea (grant: 110100713) and "Human Resource Development (advanced track for Si-based solar cell materials and devices, project number: 201040100660)" grant from the Korea Institute of Energy Technology Evaluation and Planning (KETEP) funded by the Korea government Ministry of Knowledge Economy.

REFERENCES

(1) Kaminsky, W. *Macromol. Chem. Phys.* **2008**, *209*, 459−466.
(2) Hustad, P. D. *Science* **2009**, *325*, 704−707.
(3) Robert, C.; Thomas, C. M. *Chem. Soc. Rev.* **2013**, *43*, 9392−9402.
(4) Khorasani, M.; Saeb, M.; Mohammadi, Y.; Ahmadi, M. *Chem. Eng. Sci.* **2014**, *111*, 211−219.
(5) Ahmadi, M.; Jamjah, R.; Nekoomanesh, M.; Zohuri, G.; Arabi, H. *Macromol. React. Eng.* **2007**, *1*, 604−610.
(6) Takeuchi, D. *Dalton Trans.* **2009**, *39*, 311−328.
(7) Coates, G. W.; Hustad, P. D.; Reinartz, S. *Angew. Chem., Int. Ed.* **2002**, *41*, 2236−2257.
(8) Domski, G. J.; Rose, J. M.; Coates, G. W.; Bolig, A. D.; Brookhart, M. *Prog. Polym. Sci.* **2007**, *32*, 30−92.
(9) Makio, H.; Terao, H.; Iwashita, A.; Fujita, T. *Chem. Rev.* **2011**, *111*, 2363−2449.
(10) Kempe, R. *Chem.—Eur. J.* **2007**, *13*, 2764−2773.
(11) Valente, A.; Mortreux, A.; Visseaux, M.; Zinck, P. *Chem. Rev.* **2013**, *113*, 3836−3857.
(12) Britovsek, G. J. P.; Cohen, S. A.; Gibson, V. C.; Maddox, P. J.; van Meurs, M. *Angew. Chem., Int. Ed.* **2002**, *41*, 489−491.
(13) Britovsek, G. J. P.; Cohen, S. A.; Gibson, V. C.; van Meurs, M. *J. Am. Chem. Soc.* **2004**, *126*, 10701−10712.
(14) Arriola, D. J.; Carnahan, E. M.; Hustad, P. D.; Kuhlman, R. L.; Wenzel, T. T. *Science* **2006**, *312*, 714−719.
(15) Chum, P. S.; Swogger, K. W. *Prog. Polym. Sci.* **2008**, *33*, 797−819.
(16) Pan, L.; Zhang, K.; Nishiura, M.; Hou, Z. *Angew. Chem., Int. Ed.* **2011**, *50*, 12012−12015.
(17) Valente, A.; Stoclet, G.; Bonnet, F.; Mortreux, A.; Visseaux, M.; Zinck, P. *Angew. Chem., Int. Ed.* **2014**, *53*, 4638−4641.
(18) Wang, H. P.; Khariwala, D. U.; Cheung, W.; Chum, S. P.; Hiltner, A.; Baer, E. *Macromolecules* **2007**, *40*, 2852−2862.
(19) Alfano, F.; Boone, H. W.; Busico, V.; Cipullo, R.; Stevens, J. C. *Macromolecules* **2007**, *40*, 7736−7738.
(20) Kuhlman, R. L.; Klosin, J. *Macromolecules* **2010**, *43*, 7903−7904.
(21) Murphy, V.; Bei, X.; Boussie, T. R.; Brümmer, O.; Diamond, G. M.; Goh, C.; Hall, K. A.; Lapointe, A. M.; Leclerc, M.; Longmire, J. M.; Shoemaker, J. A.; Turner, H.; Weinberg, W. H. *Chem. Rec.* **2002**, *2*, 278−289.
(22) Hustad, P. D.; Kuhlman, R. L.; Carnahan, E. M.; Wenzel, T. T.; Arriola, D. J. *Macromolecules* **2008**, *41*, 4081−4089.
(23) Zhang, M.; Carnahan, E. M.; Karjala, T. W.; Jain, P. *Macromolecules* **2009**, *42*, 8013−8016.
(24) Zhang, M.; Karjala, T. W.; Jain, P. *Ind. Eng. Chem. Res.* **2010**, *49*, 8135−8146.
(25) Zhang, M.; Karjala, T. W.; Jain, P.; Villa, C. *Macromolecules* **2013**, *46*, 4847−4853.
(26) Anantawaraskul, S.; Somnukguande, P.; Soares, J. B. P. *Macromol. Symp.* **2012**, *312*, 167−173.
(27) Mohammadi, Y.; Jabbari, E. *Macromol. Theory Simul.* **2006**, *15*, 643−653.
(28) Odian, G. *Principles of Polymerization*, 4th ed.; Wiley-Interscience: New York, 2004; p 481.
(29) Braunecker, W. A.; Matyjaszewski, K. *Prog. Polym. Sci.* **2007**, *32*, 93−146.
(30) D'Agosto, F.; Boisson, C. *Aust. J. Chem.* **2010**, *63*, 1155−1168.
(31) Benedicto, D.; Claverie, J. P.; Grubbs, R. H. *Macromolecules* **1995**, *28*, 500−511.
(32) Kim, J. W.; Lee, K. J.; Lee, H. H. *Polymer* **1998**, *39*, 2789−2793.
(33) Ventura, A.; Chenal, T.; Bria, M.; Bonnet, F.; Zinck, P.; Ngono-Ravache, Y.; Balanzat, E.; Visseaux, M. *Eur. Polym. J.* **2013**, *49*, 4130−4140.
(34) Wei, J.; Sita, L. R. *Polym. Prepr.* **2011**, *52*, 316−317.
(35) Wei, J.; Zhang, W.; Wickham, R.; Sita, L. R. *Polym. Prepr.* **2011**, *52*, 225−226.
(36) Valente, A.; Zinck, P.; Mortreux, A.; Visseaux, M. *Macromol. Rapid Commun.* **2009**, *30*, 528−531.
(37) Valente, A.; Zinck, P.; Mortreux, A.; Visseaux, M. *J. Polym. Sci., Part A: Polym. Chem.* **2011**, *49*, 1615−1620.
(38) Bhrian, N. N.; Brintzinger, H.-H.; Ruchatz, D.; Fink, G. *Macromolecules* **2005**, *38*, 2056−2063.
(39) Kuhlman, R. L.; Wenzel, T. T. *Macromolecules* **2008**, *41*, 4090−4094.
(40) Wang, L.; Broadbelt, L. J. *Macromolecules* **2009**, *42*, 7961−7968.
(41) Wang, L.; Broadbelt, L. J. *Macromolecules* **2010**, *43*, 2228−2235.
(42) Hustad, P. D.; Kuhlman, R. L.; Arriola, D. J.; Carnahan, E. M.; Wenzel, T. T. *Macromolecules* **2007**, *40*, 7061−7064.
(43) Xiao, A.; Wang, L.; Liu, Q.; Yu, H.; Wang, J.; Huo, J.; Tan, Q.; Ding, J.; Ding, W.; Amin, A. M. *Macromolecules* **2009**, *42*, 1834−1837.
(44) Shan, C. L. P.; Hazlitt, L. G. *Macromol. Symp.* **2013**, *257*, 80−93.
(45) Tong, Z.; Huang, J.; Zhou, B.; Xu, J.; Fan, Z. *Macromol. Chem. Phys.* **2013**, *214*, 605−616.